Fretting wear behaviour of Zn-Ni alloy coatings

Lisa Lee[1], Édouard Régis[2], Sylvie Descartes[2] & Richard R. Chromik[1*]

[1] Department of Mining and Materials Engineering, McGill University, Québec, Canada

[2] Université de Lyon, CNRS, INSA-Lyon, LaMCoS UMR5259, F-6962, France

* Corresponding author Email address: richard.chromik@mcgill.ca

Abstract

Cadmium coatings are used in the aerospace industry primarily as a corrosion resistant plating, but also in applications where tribological properties are also important. Due to the carcinogenic nature of Cd, many coatings have been proposed as replacements, with Zn-Ni being the leading candidate. In this study, we examine two Zn-Ni coatings with differences in their surface roughness and their content of through thickness defects, including pores and cracks. The morphological differences between the coatings had a noticeable effect on their fretting wear behaviour.

A customized tribometer, with a reciprocating rounded pin (AISI 440C steel) on flat (Zn-Ni) geometry, was used to perform fretting wear tests. The two morphologically different Zn-Ni coatings were tested at room temperature using ±70, 100 and 150 µm displacements and 133 N and 447 N constant normal loads. The surface of the wear scar was analysed using scanning electron microscopy coupled with energy dispersive X-ray spectroscopy for changes in morphology and chemistry. Wear volume was measured from surface profiles obtained using confocal microscopy.

Hysteresis fretting loops of the tests showed that for both coatings, at ±70 µm displacement remains in no slip condition, at ±100 µm in the mixed slip condition, and at ±150 µm displacement remains in gross slip condition. Although the coatings had similar stick-slip behaviour, the smoother coating has a slower progression of wear from the no slip to gross slip conditions than the rougher coatings. Also, differences in the wear scar morphologies are attributed to the differences in the coating morphologies, which resulted in different wear and velocity accommodation mechanisms.

Keywords: Fretting, Electrodeposited Coatings, Surface morphology, Intermetallics

1. Introduction

Zn-Ni alloy coatings are used in the aerospace and automotive industry for corrosion protection coatings of steel. They were developed in the 1980's as a replacement for cadmium coatings due to the carcinogenic and toxic nature of cadmium [1-3]. There are numerous corrosion properties studies of Zn-Ni coatings in the open literature, such as those found in [3-9]. However, these coatings are also used where tribological properties are critical to the performance, such as landing gear components and steel fasteners. Research on the tribological properties are fewer and focus on the sliding wear properties [7, 10-12]. Fretting wear properties of Zn-Ni coatings are also not widely studied although damages due to fretting are observed in aerospace assemblies, especially in joints, fasteners and tight fitting assemblies.

Fretting occurs when two surfaces are in relative oscillatory motion at very small amplitudes [13]. Vingsbo [14] divided fretting into three different regimes (1) stick, (2) mixed stick-slip and (3) gross slip. The stick regime can be obtained through fretting at very low displacement amplitudes and is characterized by mild asperity wear with unworn material between the contact junctions. The mixed stick-slip regime is characterized by a central area mildly worn area due to sticking of the counterface, which is surrounded by a highly worn area where slipping of the counterface occurs. The gross slip regime can be obtained through fretting at relatively large displacement amplitudes and is characterized by severe wear and sliding wear marks are observed. Ramalho *et al.* [15] compared the fretting fatigue behaviour of electrodeposited zinc coated steel with uncoated steel. They found that zinc coatings markedly improved the wear resistance and fretting fatigue life of steel and observed much less adhesive wear and oxidation in the wear scars in the coated samples. Gao *et al.* [16] observed the fretting fatigue properties of Ni-P coated steel, and found that Ni-P coatings improved the fretting fatigue resistance of mild strength steels by modifying the tribobehaviour of the substrates due to the high hardness of Ni-P coatings.

Tribological properties are not intrinsic to a material, but rather are dependent on many conditions such as coupled materials, surface roughness, temperature, humidity, etc. Commercially available Zn-Ni alloy coatings are mostly electrodeposited on the substrates and depending on the electrodeposition conditions, the surface morphology can differ for similar compositions. With other test and material parameters kept similar (normal load, humidity, material composition, etc.), surface morphology and roughness can have a strong effect on the tribological properties. In early studies of fretting wear by Waterhouse [17], the effects of roughness on the surface damage due to wear showed that a rougher surface suffered less fretting damage than a better surface finish. This was attributed to two mechanisms: a rough surface is able to "take-up more tangential movement" due to a higher plasticity index and work hardening of asperities, and also wear debris, which can contribute to higher wear rate, can be removed from the contact by falling into the hollows of the surfaces [17]. More recently, Kubiak *et al.* [18] studied the effects of surface roughness on the fretting behaviour of AISI 1034 steel and Ti-6Al-4V and found that with rougher surfaces, the CoF is lower and the wear rate is higher in both material systems.

In this study, two Zn-Ni alloy coatings from different commercially available sources with different surface morphologies were subjected to fretting in order to evaluate the effects of surface morphology. By varying the displacement amplitude, contact conditions under the stick, mixed slip and gross slip regimes were achieved. The coatings were tested under the three regimes in order to compare their fretting wear behaviours by observations of the fretting loops and wear scars through SEM imaging and profilometry.

2. Methods

2.1 Coating Deposition

Two commercially available zinc-nickel alloy coating were used for this study. Zinc-nickel alloy coating was deposited on 100 x 160 mm, 0.8 mm thick low carbon steel (SAE 1006). The coatings were deposited using 2 commercially available plating processes in an industrial pilot plating tank as follows:

For C-ZnNi, an alkaline NaOH (120-135 g/L) based plating solution which contains zinc (7-10 g/L), Nickel (1-1.8 g/L) was used. The plating operation was performed at 21-25 °C with a current density of 10 mA/cm^2. The as plated samples were then passivated using a blue trivalent chrome passivate and then baked at 200 °C for 24 hours [19, 20].

For D-ZnNi, an alkaline NaOH (135 g/L) solution was used with Zn and Ni metal concentration maintained at 10-11:1 ratio and the pH maintained at 12-13.5. The plating operation was performed at 25 °C with a plating density of 50 mA/cm^2. The substrates were plated for 20 minutes in order to obtain a coating thickness between 15-20 μm. Prior to plating, the substrates were grit blasted and acid pickled using HCl. The plated samples were passivated using a blue trivalent conversion coating and baked at 200 °C for 24 hours [9].

An electron probe micro-analyzer (EPMA) test was performed on the coatings in order to assess the coating composition, and C-ZnNi contained 14.63wt% ±0.05 Ni and D-ZnNi contained 15.65wt% ±0.58 Ni. Standards of zinc and zinc sulfide were used to assess the content of zinc and standards of nickel and nickel oxide were used to assess nickel content. The higher standard deviation in D-ZnNi coatings is due to higher surface roughness.

2.2 Characterization

The morphologies of the coatings were observed using scanning electron microscopy (SEM) in their as prepared and post-wear states. Chemical composition of the wear scars and transfer films were obtained through energy dispersive x-ray spectroscopy (EDX). SEM and EDX were performed using a FEI Quanta 600 microscope with a tungsten filament source. An accelerating voltage of 20kV was used. Selected specimens were observed in cross section and were cut with a diamond blade and prepared metallographically.

X-ray diffraction (XRD) was used to confirm the phase of the coating. A Bruker Discover D8-2D, fitted with a Co-Kα source, was used in the standard θ-2θ mode on the unworn coatings. Profilometry was performed on the wear scars. An Altisurf 500 confocal microscope coupled with Phénix 2 software was used to obtain the profile maps.

Mechanical properties of the coatings were determined using nanoindentation with a Ubi3 nanoindenter (Hysitron Incorporated, Minneapolis, MN, USA) and a diamond Berkovich tip. Indentation was carried out on cross sections of the coatings with a peak load of 5 mN, a loading/unloading rate of 1 mN/s and 2 second hold time at peak load. Hardness and elastic modulus were calculated using the Oliver and Pharr method [21].

2.3 Fretting wear test

Fretting wear tests were performed using a custom built tribometer at Laboratoire de Mécanique des Contacts et des Structures (LaMCoS, INSA, Lyon, France). An AISI 440C steel counterface with a 20 mm curvature was used. Two initial loads were used to evaluate the coating: 133 N and 447 N. Using a Young's Modulus of 118 GPa and Poisson's Ratio of 0.23 for Zn-Ni [22, 23], this corresponds to an initial Hertzian contact stress of 740 MPa and 1110 MPa and a Hertzian contact radius of 292 μm and 439 μm, respectively. In order to evaluate the stick-slip behaviours, tests were run with frequency of 15 Hz and displacement amplitudes of ±70, 100 and 150 μm. In doing so, the degree of exposure of the contact area to the environment will be different (Figure 1). As some of the motion can be taken up by the first bodies and structure, the imposed displacement amplitudes will not be the same as the actual slip in the contact [24]. The tests were performed in ambient temperature (23-25 °C) and humidity (35-40% relative humidity). Measurements of the tangential force, normal force and displacement were recorded throughout the test.
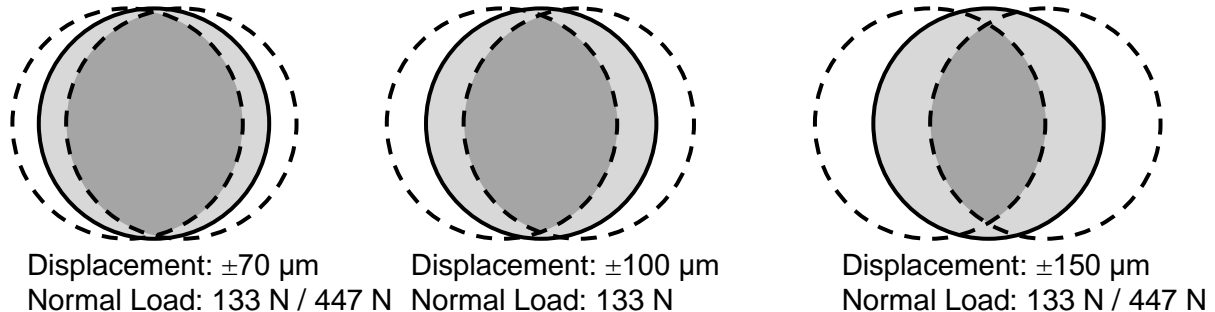

Displacement: ±70 μm
Normal Load: 133 N / 447 N

Displacement: ±100 μm
Normal Load: 133 N

Displacement: ±150 μm
Normal Load: 133 N / 447 N

Figure 1. Schematic of theoretical contact exposure to environment
Light gray = original contact area, Dark gray = Unexposed area

3. Results
3.1 Coating Characterization

SEM micrographs of the two different types of coatings for the surface morphology and cross sectional morphology are shown in Figure 2. From the surface morphology, C-ZnNi coatings shows a smooth surface formed through fine platelets, with gradual rises and falls. No through thickness porosity is evident on the surface morphology. However, in the cross section, although the coating appears well adhered to the substrate, through thickness cracks and small porosities are observed. D-ZnNi coatings are formed through agglomeration of platelets in hemispherical shapes, which forms hills and valleys with steep slopes, causing large through thickness porosities from the surfaces. Cross-sections of the coating shows good adhesion of

the coating to the substrate. Small porosities and cracks along the agglomerations are observed. The differences of the surface morphologies has an effect on the surface roughness. C-ZnNi has the lower roughness (1.35μm $\pm$ 0.19 R_a) while D-ZnNi has the higher roughness (2.90μm $\pm$ 0.35 R_a). In both coatings, through thickness defects are observed which allows trapped hydrogen from the electrodeposition process to escape from the substrate to the environment during a subsequent baking process at 200 °C, making it less susceptible to hydrogen embrittlement [8, 25].

XRD was performed on the as received coatings in the standard θ-2θ mode, and both diffraction patterns are shown in Figure 3. Both coatings show peaks corresponding to γ-ZnNi despite the differences in the intensities of the peaks. The discrepancies in the intensities of the peaks may be due to differences in surface morphology and crystallographic orientation.

Nanoindentation on the cross sections of the coatings showed small differences between the mechanical properties. The reduced elastic modulus were similar, E_r = 127 $\pm$ 15 GPa for C-ZnNi and 137 $\pm$ 12 GPa for D-ZnNi. However, the hardness of the C-ZnNi coating (H = 5.2 $\pm$ 0.3 GPa) was smaller than that for the D-ZnNi coating (H = 6.6 $\pm$ 0.3 GPa). The differences in hardness may be attributed to the slightly higher Ni content in D-ZnNi coatings, but may also be related to differences in the crystallographic orientation.
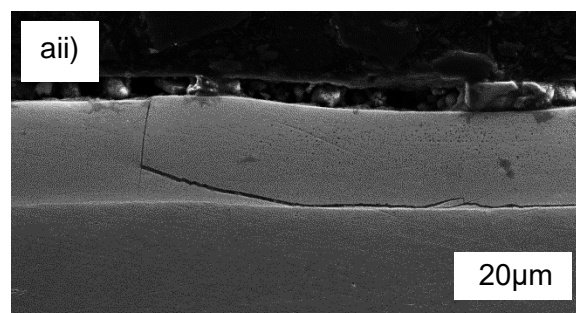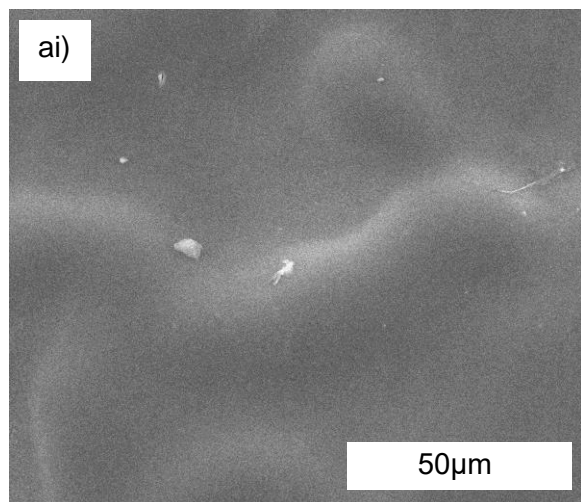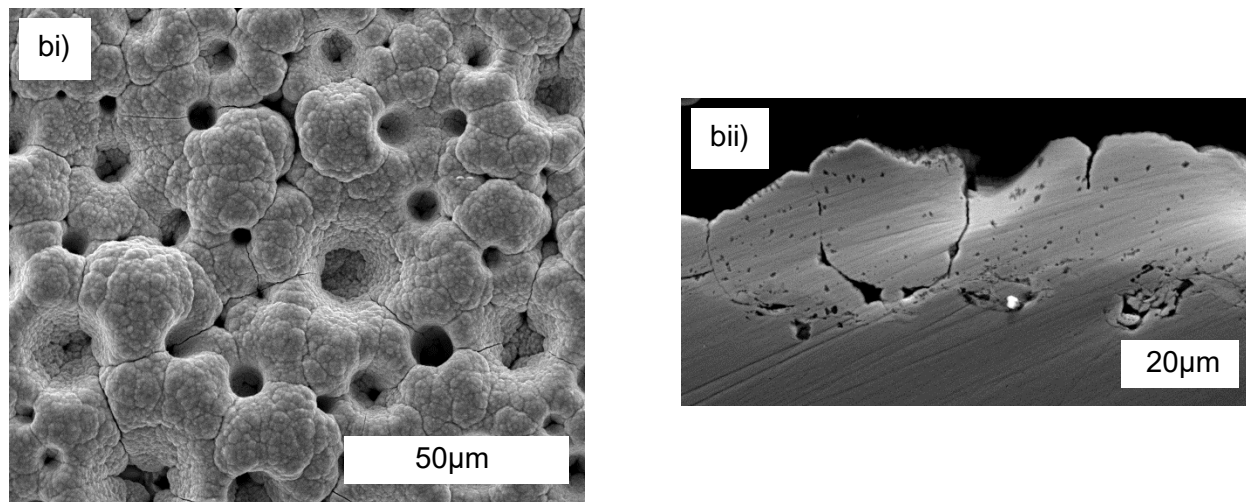
Figure 2. a) C-ZnNi and b) D-ZnNi SEM images of i) surface morphology ii) cross section
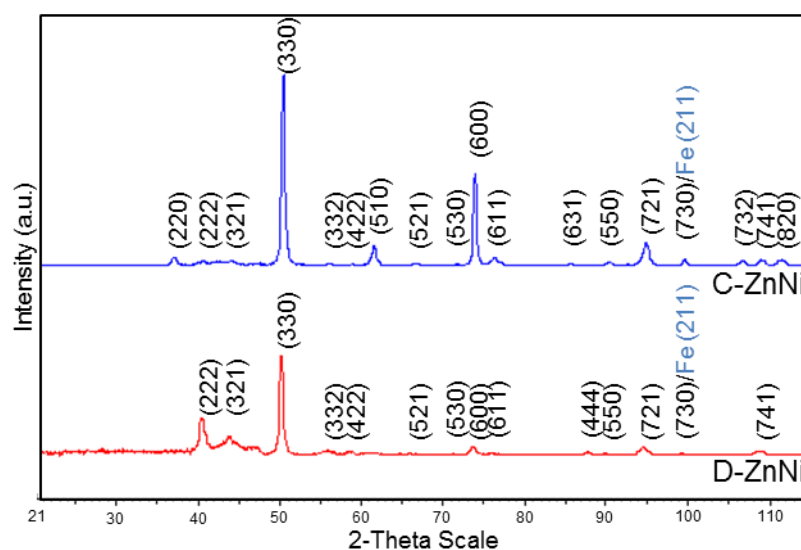

Figure 3. Diffraction pattern of C-ZnNi and D-ZnNi

3.2 Fretting Wear Test

Plotting the tangential force versus the tangential displacement gives the fretting wear hysteresis loop, which provides information on the stick-slip phenomena. The area enclosed by the loop (Figure 4) is indicative of the dissipated energy due heat, noise, material structure transformation, chemical reactions and third body behaviour [26, 27]. Fretting hysteresis loops for stick regime shows a closed loop indicating very little wear occurs in this regime as little energy is lost. For the gross slip regime, a trapezoidal loop is observed due to the large amount of energy dissipated often associated with wear [13, 26, 27].
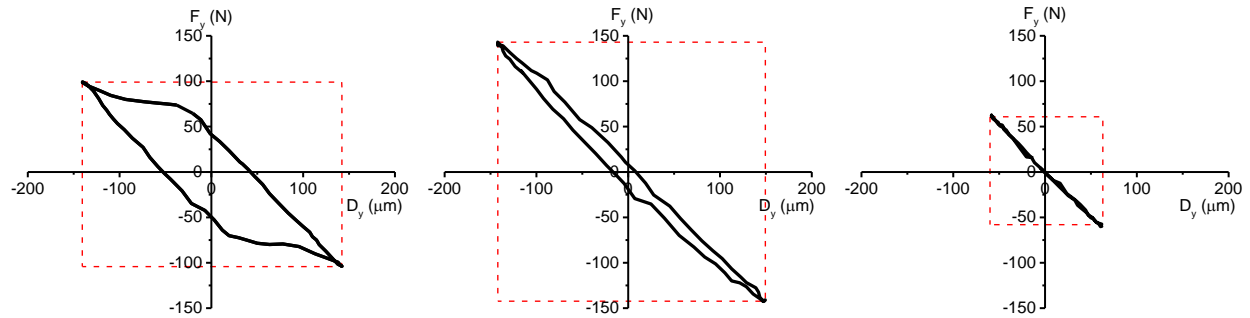
**Figure 4. Typical shapes of a) trapezoidal, b) elliptical and c) closed fretting loops from tests**

Figure 4 shows examples of trapezoidal, elliptical and closed fretting loops from typical data obtained from the tests. The energy ratio is defined as the dissipated energy (E_d) over the total energy (E_t) from the fretting loops [28]. The energy ratio (E_d/E_t) of the tests are plotted versus the number of cycles in order to observe the evolution of the fretting wear regimes over time for every 225 cycles (see Figure 5). When the energy ratio lies below 0.2, the fretting wear regime is defined as the stick regime, whereas above 0.2 is the gross slip regime [28]. For a normal load of 133 N and a displacement amplitude of ±70 µm, D-ZnNi coatings shows an energy ratio below 0.2 and closed fretting loops throughout the tests (Figure 5a), indicating stick behaviour at the contact at these conditions. In contrast, for C-ZnNi coatings, the energy ratio went slightly above 0.2 in the initial cycles, and fretting loops were open and trapezoidal in shape. However the energy ratio quickly stabilized after 2000 cycles to values below 0.2 and the fretting loops became closed (Figure 5a). This indicates that in the initial 2000 cycles C-ZnNi showed slip behaviour and after 2000 cycles exhibited stick behaviour until the end of the test. Looking at the wear scar depths shown in Figure 6, both coatings showed shallow wear scar depths, indicating mild amount of wear.

The energy ratio and fretting loops for tests performed with displacement amplitude of ±100 µm and 133 N normal load are shown in Figure 5b. In both coatings, the energy ratio starts above 0.2 and with an open trapezoidal fretting loop and transitions to an energy ratio below 0.2 with a closed fretting loop, indicating mixed slip behaviour. The transition time for C-ZnNi is earlier than D-ZnNi. C-ZnNi also shows a gradual transition to the stick behaviour whereas for D-ZnNi the transition is much more abrupt and also shows a more erratic behaviour in the earlier cycles with multiple transitions between the sticking and slipping behaviour, which is indicated by the opening and closing of the fretting loops and fluctuating energy ratios. Figure 6 of the wear scar depth also shows a deeper wear scar with D-ZnNi than with C-ZnNi, indicating that moderate wear occurred with D-ZnNi, whereas for C-ZnNi only mild wear occurred.
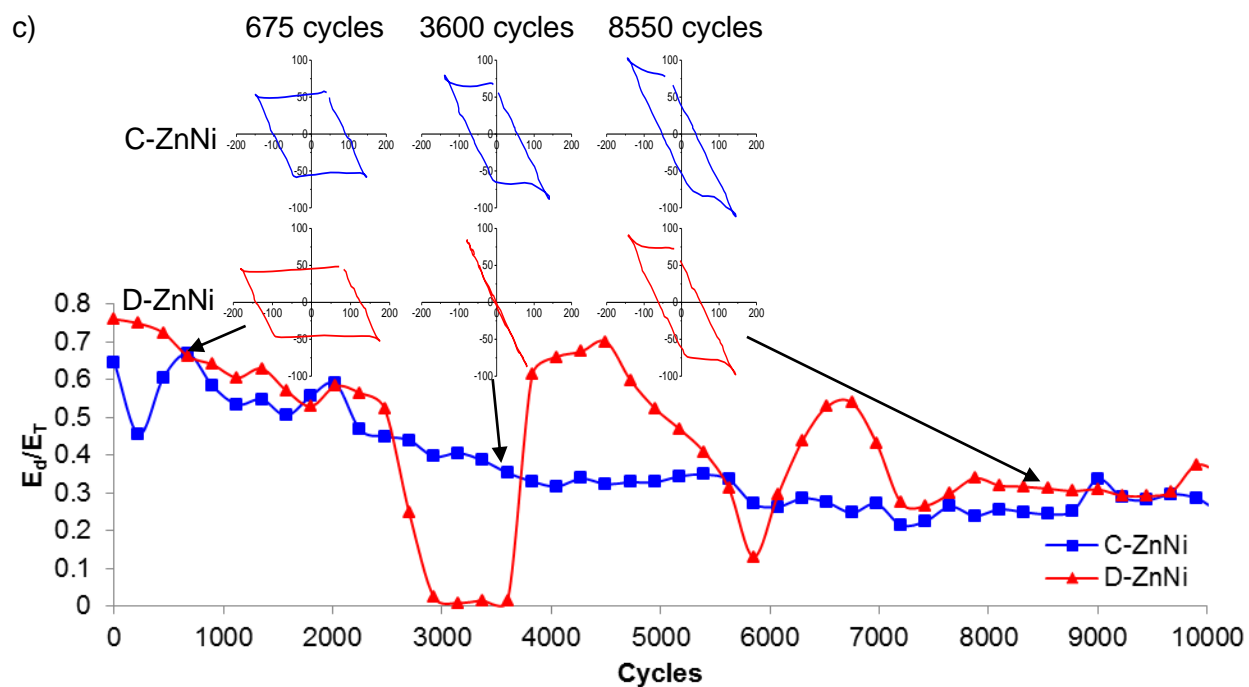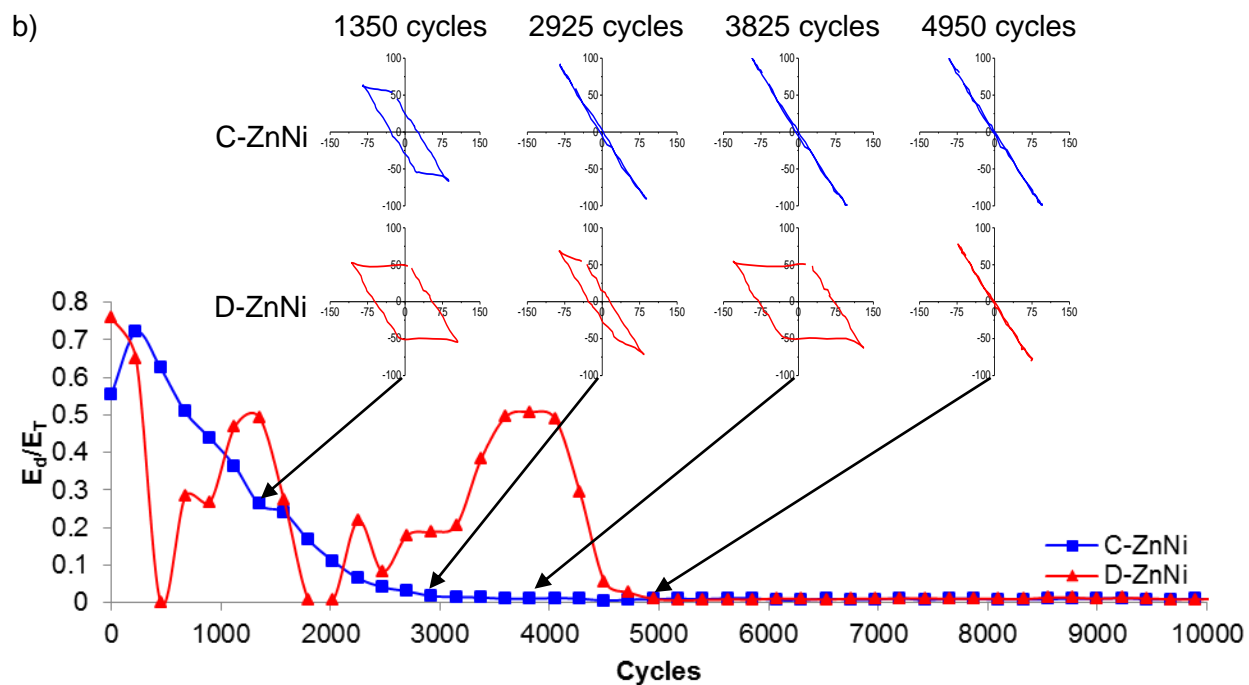
At ±150 µm displacement amplitude and 133 N normal load tests, a high energy ratio and open trapezoidal fretting load prevails throughout the tests for the 2 coatings, shown in Figure 5c. This indicates a gross slip regime throughout the tests. A drop in the energy ratio due to closed fretting loop is observed in D-ZnNi at around 3000 cycles, whereas for C-ZnNi, the evolution of the energy ratio and fretting loop shapes are more constant. From the wear scar

depth shown in Figure 6, although the wear depths are large for both coatings, D-ZnNi shows a larger wear depth than C-ZnNi.

For the normal load of 447 N in both ZnNi coatings, tests with displacement amplitudes of ±70 µm fretting loops were closed throughout the test, resulting in an energy ratio well below 0.2 and in the stick regime. Increasing displacement amplitudes to ±150 µm showed elliptical fretting loops and a higher energy ratio (C-ZnNi 0.063 ± 0.004, D-ZnNi 0.069 ± 0.001) indicating partial slip behaviour. Shallow wear scar depths were observed for displacement amplitudes of ±70 µm and ±150 µm for both coatings, indicating mild amounts of wear.
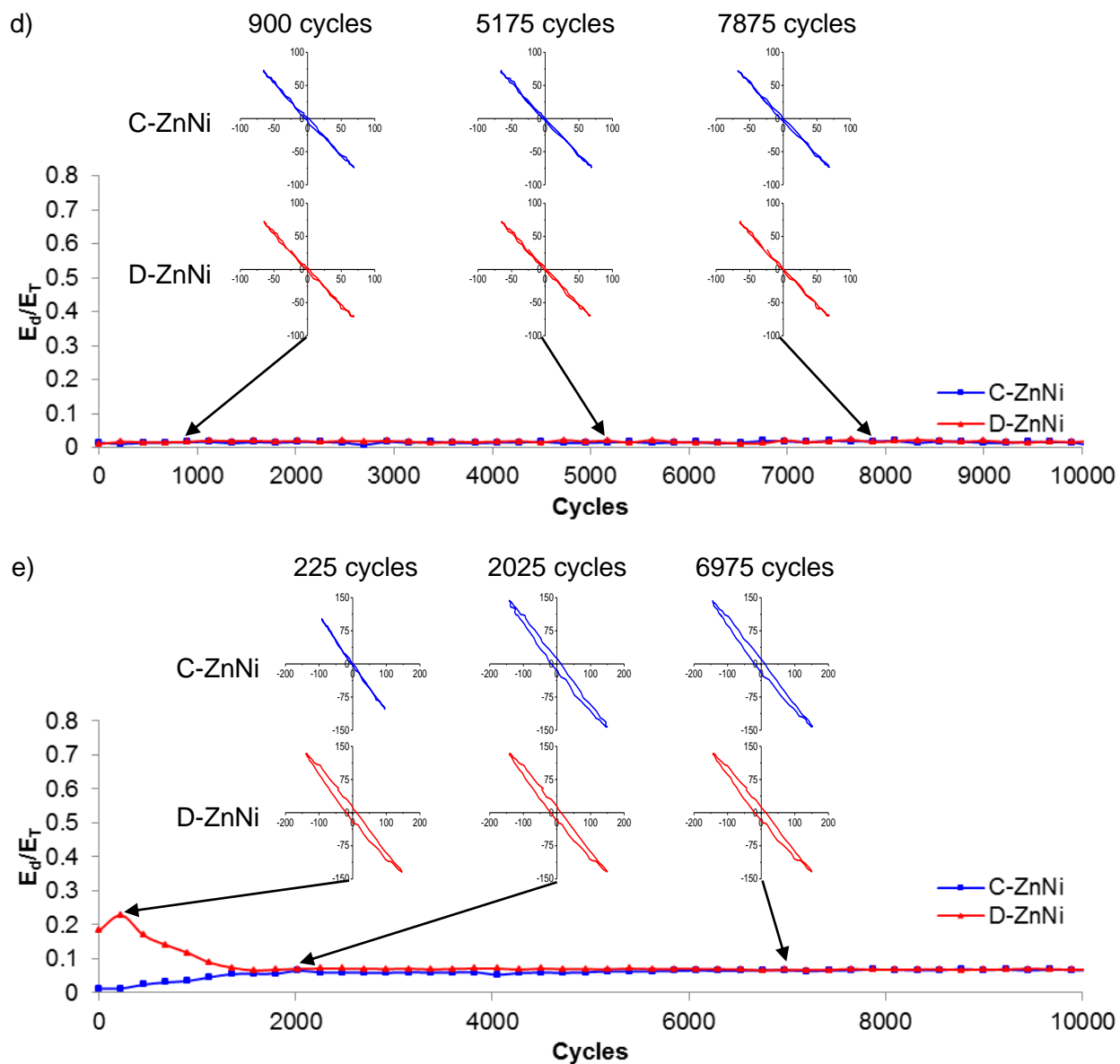
b)

c)
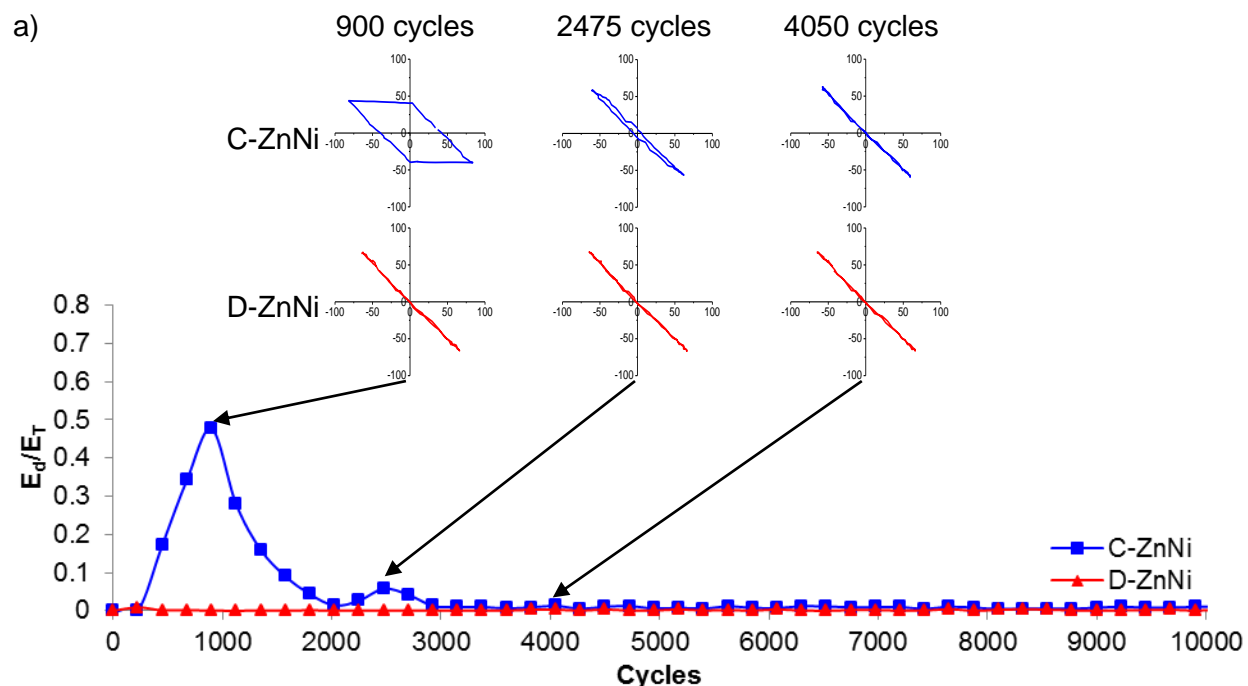
Figure 5. Energy ratio evolution of C-ZnNi and D-ZnNi at a) ± 70 µm b) ± 100 µm and c) ± 150 µm displacement amplitude and 133 N normal load and d) ± 70 µm and e) ± 150 µm displacement amplitude and 447 N normal load for 10000 cycles
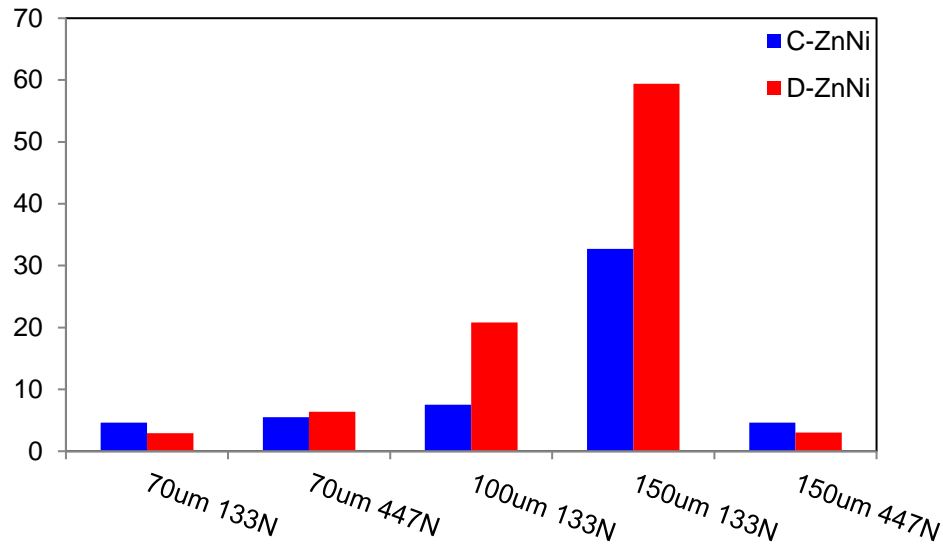
Figure 6. Fretting wear scar depths of C-ZnNi and D-ZnNi after 10000 cycles of wear

3.3 Ex situ wear scar analysis

SEM images of the wear scars were obtained post fretting wear test and are shown in Figure 7-12. Tests with displacement amplitude of ±70 μm and 133 N normal load after 10000 cycles are shown in Figure 7, where only mild wear occurred in both coatings. C-ZnNi coatings (Figure 7a) show more wear particles at this condition. This may be due to slip occurring at the beginning of the test where the energy ratio rises above 0.2 before stabilizing to near zero values (Figure 5a). The wear scar is characterized by plastic flow and small regions of unworn coating in a central region, and delamination and oxidized wear particles at the edge of the contact and the periphery. The counterface of the C-ZnNi coating shows transferred material at the center and oxidized wear debris adhering to the sides. D-ZnNi coatings (Figure 7b) show less wear debris compared to C-ZnNi. Slight deformation of the asperities is observed and small oxidized wear particles are observed at the hollows of the coating. This is in agreement with the near zero energy ratio and closed fretting loops throughout the test observed in Figure 5a. Wear debris are not observed on the counterface of D-ZnNi coatings test and instead gouges are observed.
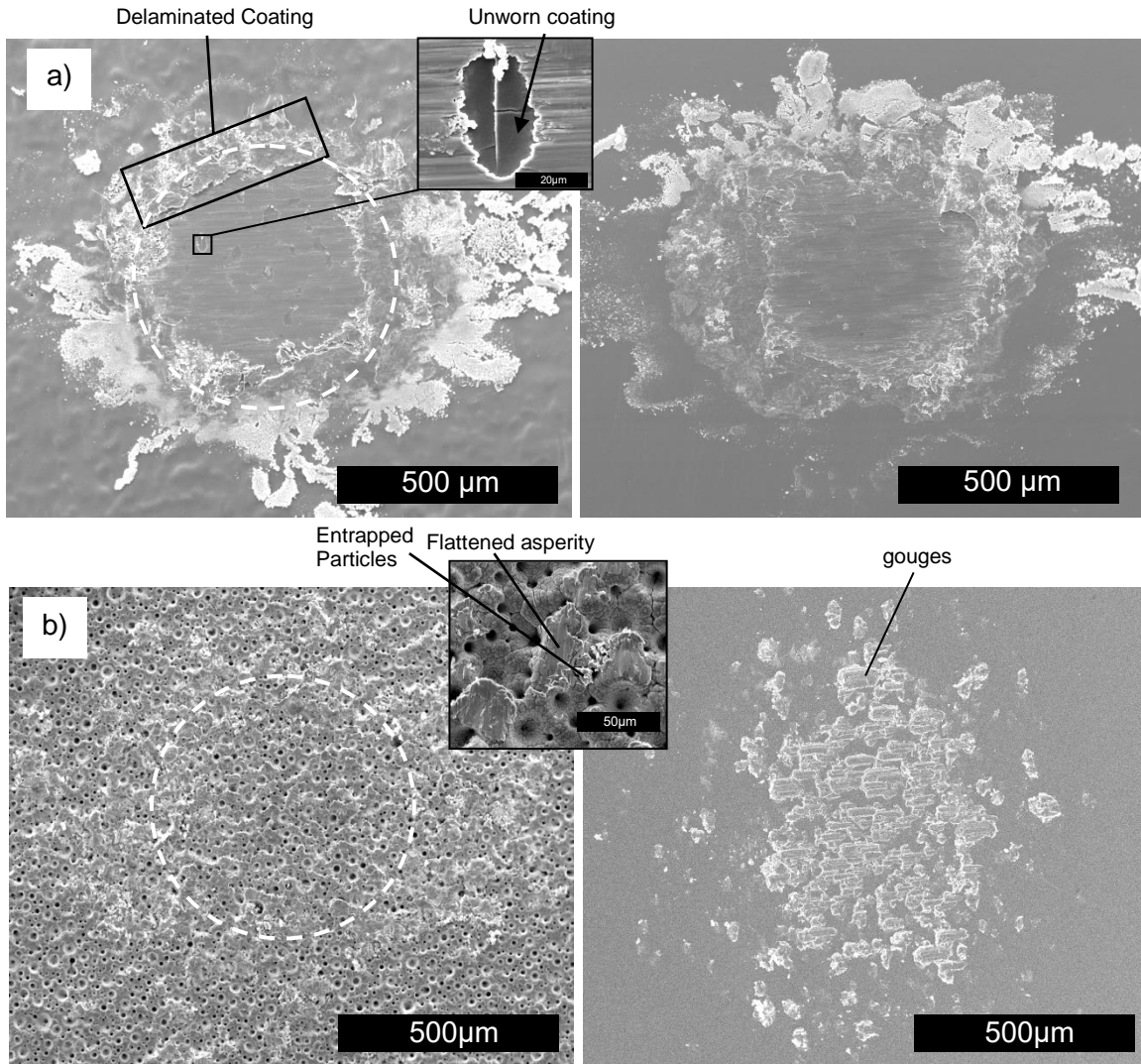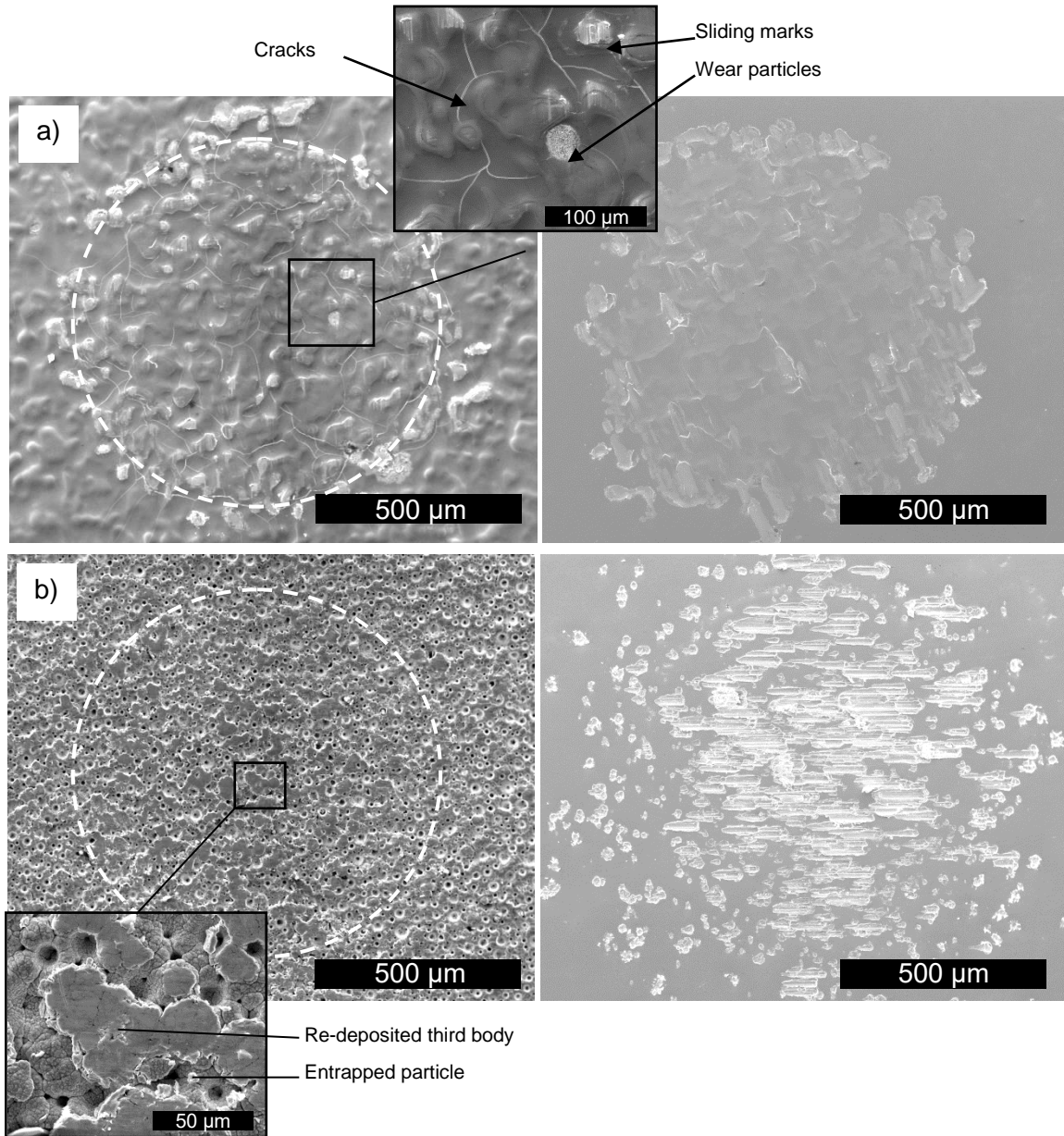
Figure 7. Fretting wear scar (left) and counterface (right) at contact condition of 133 N normal load and ±70 µm displacement amplitude after 10000 cycles a) C-ZnNi and b) D-ZnNi. Sliding direction ↔

Figure 8 show the tests performed at ±70 µm displacement amplitude and 447 N normal load. After 10000 cycles, minimal wear and only slight wearing of the asperities are observed for both coatings. For C-ZnNi coatings (Figure 8a), cracks formed in the contact area. Junctions where the coating and counterface meets appears to be worn off and small oxide particles reside within the worn junctions. Some sliding marks are also observed inside the wear scar, indicating plastic flow of material. At the edge of the contact area, more wear particles are observed than at the central region of the wear scar. Smearing occurred on the counterface where it was in contact with the C-ZnNi coatings. D-ZnNi coatings (Figure 8b) underwent asperity wear through plastic deformation. Wear particles are also observed in the hollows of the coating. There also appears to have re-deposited wear particles on the worn asperities. Oxidized small wear particles were observed in the edge of the contact area. Similar wear scar morphologies but slightly more severe wear and larger oxide particles at the edge of the wear

scar were observed when increasing the displacement amplitude to ±150 µm. Gouges formed where the asperities of D-ZnNi coatings were in contact with the counterface.


Figure 8. Fretting wear scar (left) and counterface (right) at contact conditions of 447 N normal load and ±70 µm displacement amplitude after 10000 cycles a) C-ZnNi and b) D-ZnNi. Sliding direction ↔

Increasing the displacement amplitude from ±70 µm to ±100 µm at a normal load of 133 N caused an increase in wear for both coatings, as seen by observation of the wear scars and counterfaces in Figure 9-10. After 10000 cycles, C-ZnNi (Figure 9a) and D-ZnNi (Figure 10a) coatings both showed plastically deformed material at the central region of the wear scar

surrounded by chunks of detached material and oxidized wear particles in the annular area
around the central region (Figures 9b2 and 10b1.

Difference between the C-ZnNi and D-ZnNi coatings for ±100 µm and 133 N load was
the shape of the extruded wear particles, as with C-ZnNi coatings, flatter flake-like compacted
oxides formed, while with D-ZnNi coatings, thin flakes-like compacted oxides were formed
(Figures 9b1 and 10b2). At the center of the wear scar for C-ZnNi coatings, EDX showed no
iron peaks (Figure 9c), indicating a layer of coating material is still present. D-ZnNi coatings
have the larger wear scar and EDX at the center shows presence of iron but not chromium,
which may indicate substrate exposure rather than sources of iron from the counterface. These
observations are consistent with the wear scar depths (Figure 6). D-ZnNi shows a higher wear
depth which is slightly larger than the coating thickness, whereas C-ZnNi shows a moderate
wear depth which is lower than the coating thickness. Thus substrate exposure is more likely for
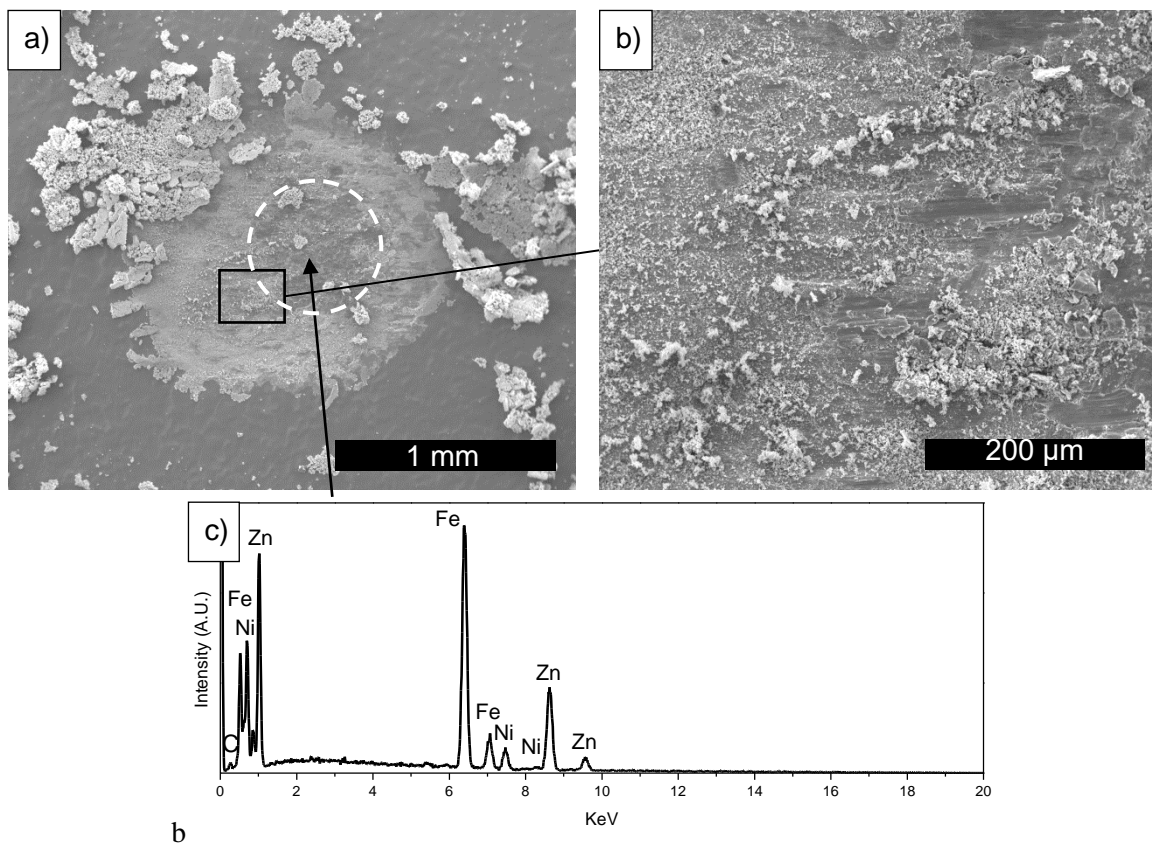D-ZnNi than C-ZnNi.
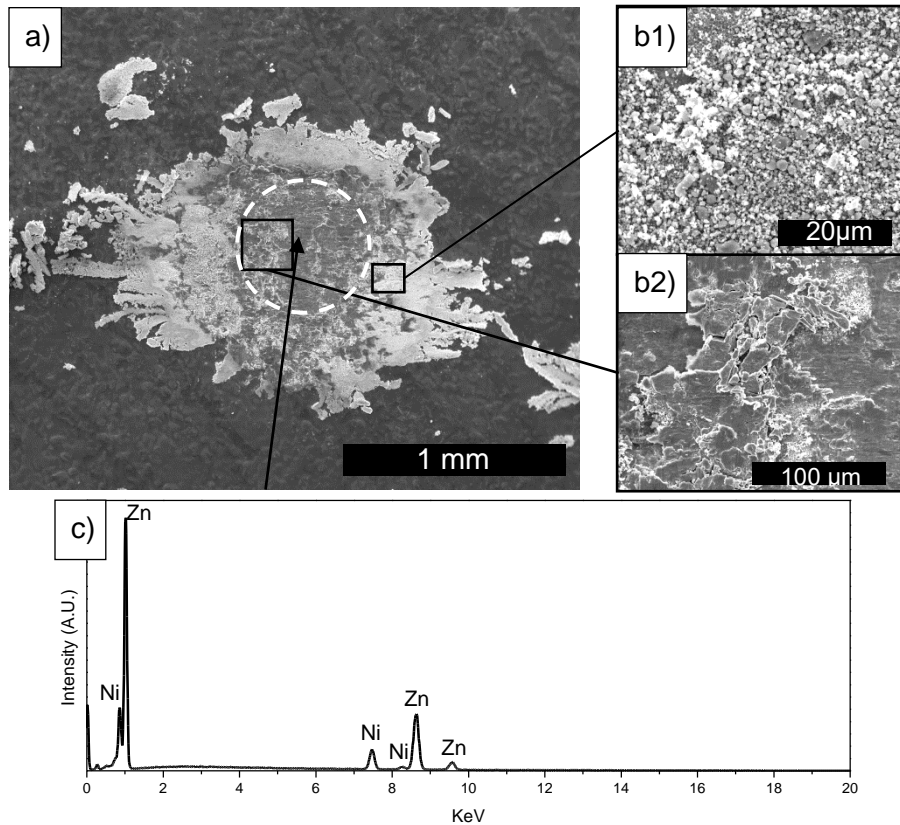
Figure 9. a) Fretting wear scar, b) third body morphology and c) EDX spectrum of center area of C-ZnNi coating at contact conditions 133 N normal load and ±100 µm displacement amplitude after 10000 cycles. Sliding direction ↔
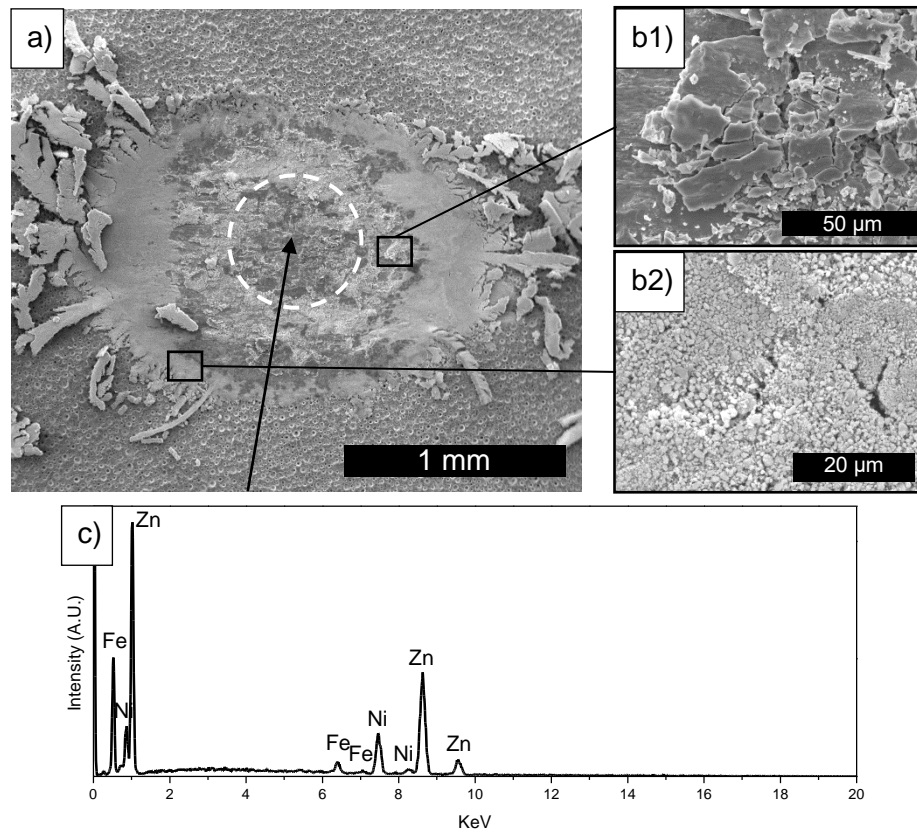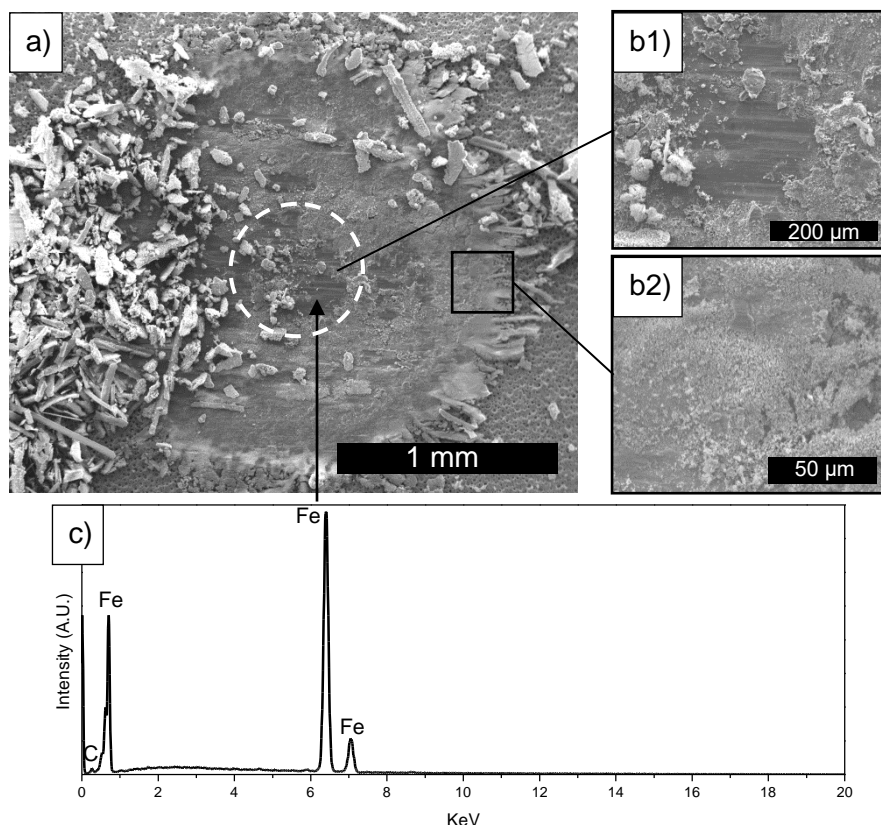
Figure 10. a) Fretting wear scar, b) third body morphology and c) EDX spectrum of center area of D-ZnNi coating at contact conditions 133 N normal load and ±100 μm displacement amplitude after 10000 cycles. Sliding direction ↔

Tests performed at ±150 μm displacement amplitude and 133 N normal load showed severe wear in all cases after 10000 cycles (Figure 11-12). Oxide particles are present throughout the contact except for small patches of areas where plastic flow of material is observed. In the patches, C-ZnNi coatings (Figure 11a) show plastic flow of material in the patch area. Chunks of detached material and re-deposited third bodies are also observed near the edge of the patch area shown in the inset image. For D-ZnNi coating, deformation due to sliding is observed in the patch, with re-deposition of third bodies. Substantial amount of wear debris was extruded out of the wear scar. Extruded wear debris from D-ZnNi coatings shows small particles compacted into thin flake-like shapes and are more abundant, whereas for C-ZnNi coatings, extruded debris are flat and more flake-like. For both coatings at this condition, intense iron peaks were found at the center of the wear scars (Figure 11-12b) with EDX. This indicates substrate exposure and is in agreement with the wear scar depth (Figure 6), which were much higher than the coating thickness. C-ZnNi coatings showed small intensity zinc and nickel peaks, indicating that some coating material remained in the center of the contact, whereas D-ZnNi coating showed no zinc and nickel peaks, indicating complete removal of the coating. The abundance of wear particles and sliding marks in the central region indicate that both coatings were in the gross slip regime.

b

Figure 11. a) Fretting wear scar b) third body morphology and c) EDX spectrum of center area of C-ZnNi coating at contact conditions 133 N normal load and ±150 µm displacement amplitude after 10000 cycles. Sliding direction ↔

Figure 12. a) Fretting wear scar b) third body morphology and c) EDX spectrum of center area of D-ZnNi coating at contact conditions 133 N normal load and ±150 µm displacement amplitude after 10000 cycles. Sliding direction ↔

4. Discussion

The fretting wear behaviour of two ZnNi coatings with different surface morphologies was studied under various contact conditions including the stick, mixed slip and gross slip. In the stick regime, cracks formed in C-ZnNi as a method of velocity accommodation, where through-thickness cracks formed columns in the smooth, compact coating, making it easier to flex [29]. In contrast, D-ZnNi did not form any cracks and the coating's nodular surface morphology allowed for velocity accommodation easier than a smooth, compact coating (e.g. C-ZnNi). Plastic deformation at the tops of the nodules was observed, similar to the wear behaviour of rough surfaces discussed by Waterhouse [17]. Zn and Ni were present in patches on the counterface and indicated adhesion between the top of the nodules and the steel counterface. This adhesive process was identified by Berthier as a velocity accommodation mechanism through plastic deformation of asperities [29].

In the gross slip regime, despite a higher coating hardness, more severe wear occurred for D-ZnNi than C-ZnNi although increase in hardness improves fretting wear favourably [30-32]. Higher wear in D-ZnNi than C-ZnNi may be attributed to the difference in surface morphology and roughness of the coatings. Kubiak *et al.* [18] found that in the gross slip regime, a higher roughness is associated with a higher wear rate. Also both ZnNi coatings had through thickness

defects, but defects for C-ZnNi were more vertical cracks, whereas defects in D-ZnNi, small porosities and cracks along the platelet agglomerations. Although the morphology in D-ZnNi coatings facilitates tangential motion in the stick regime, it also facilitated asperity detachment during sliding, which led to the larger wear track depth and greater amount of wear debris found around the wear scar.

In the mixed slip regime, crack formation and particle detachment competed to accommodate motion [33]. Substantial amount of wear debris in both coatings in the mixed slip regime (Figure 9a &10a) indicates particle detachment [33]. Patches of deformed material at the center of the wear scar indicates that plastic flow of material occurred where the counterface was stuck to the wear track. Both coatings transition from gross slip to stick (Figure 5b). Traversing from gross slip to stick indicates that particle detachment occurs before plastic deformation as velocity accommodation mechanisms. Higher wear rate of D-ZnNi coating is observed as the morphology of the coating facilitates particle detachment during sliding.

5. Conclusion

Differences in surface morphology contributed to a difference in fretting wear behaviour between two ZnNi coatings. C-ZnNi coatings had a much smoother surface with gradual sloped peaks and low surface roughness, whereas D-ZnNi had a much rougher surface with steep sloped peaks and large through thickness pores. Through thickness cracks were observed in both coatings, but cracks in D-ZnNi appeared to go along the platelet agglomerates, making them easier to detach during sliding. In high load tests, although both coatings remained in the stick regime, the morphologies of the wear scars were different due to differences in their wear and velocity accommodation mechanisms, which were directly tied to differences in the surface morphologies of the coatings. Cracks and plastic deformation was observed in the junctions were observed for C-ZnNi. In contrast, with D-ZnNi, due to large surface porosities, plastic deformation and asperity detachment was observed in the junctions between the counterface and the coating. Wear particles were also observed in the hollows of the coating. At low loads and small displacement amplitudes, the both coatings remained in the stick regime, but wear scar morphology were completely different from one coating to the other. For C-ZnNi, small oxidized wear particles were extruded out of the wear scars and mild delamination occurred. For D-ZnNi, wear was similar to that observed at high loads. Low loads and high displacement amplitudes allowed slipping between the contacts. D-ZnNi coatings had a much deeper wear scar and more oxidized wear particles than C-ZnNi coatings, which may be attributed to the surface morphology of D-ZnNi coatings, as the agglomerates are easier to remove than the compact C-ZnNi coating.

6. Acknowledgements

7. References

[1] M. Bielawski, Alternative technologies and coatings for electroplated cadmium and hard chromium, Canadian Aeronautics and Space Journal, 56 (2010) 67-80.

[2] Cadmium REACH Consortium, Cadmium REACH, Cadmium REACH, Brussels.

[3] G.D. Wilcox, D.R. Gabe, Electrodeposited zinc alloy coatings, Corrosion Science, 35 (1993) 1251-1258.

[4] K.R. Baldwin, C.J.E. Smith, Advances in replacements for cadmium plating in aerospace applications, Transactions of the Institute of Metal Finishing, 74 (1996) 202-209.

[5] T.V. Byk, T.V. Gaevskaya, L.S. Tsybulskaya, Effect of electrodeposition conditions on the composition, microstructure, and corrosion resistance of Zn-Ni alloy coatings, Surface and Coatings Technology, 202 (2008) 5817-5823.

[6] A. Conde, M.A. Arenas, J.J. de Damborenea, Electrodeposition of Zn-Ni coatings as Cd replacement for corrosion protection of high strength steel, Corrosion Science, 53 (2011) 1489-1497.

[7] K.R. Sriraman, S. Brahimi, J.A. Szpunar, J.H. Osborne, S. Yue, Tribocorrosion behavior of Zn, Zn-Ni, Cd and Cd-Ti electrodeposited on low carbon steel substrates, Surface and Coatings Technology, 224 (2013) 126-137.

[8] K.R. Sriraman, S. Brahimi, J.A. Szpunar, S. Yue, Hydrogen embrittlement of Zn-, Zn-Ni-, and Cd-coated high strength steel, Journal of Applied Electrochemistry, (2013) 1-11.

[9] K.R. Sriraman, S. Brahimi, J.A. Szpunar, J.H. Osborne, S. Yue, Characterization of corrosion resistance of electrodeposited Zn-Ni Zn and Cd coatings, Electrochimica Acta, 105 (2013) 314-323.

[10] S. Ghaziof, W. Gao, Electrodeposition of single gamma phased Zn-Ni alloy coatings from additive-free acidic bath, Applied Surface Science, 311 (2014) 635-642.

[11] C.N. Panagopoulos, K.G. Georgarakis, P.E. Agathocleous, Sliding wear behaviour of zinc-nickel alloy electrodeposits, Tribology International, 36 (2003) 619-623.

[12] K.R. Sriraman, H.W. Strauss, S. Brahimi, R.R. Chromik, J.A. Szpunar, J.H. Osborne, S. Yue, Tribological behavior of electrodeposited Zn, Zn-Ni, Cd and Cd-Ti coatings on low carbon steel substrates, Tribology International, 56 (2012) 107-120.

[13] G.W. Stachowiak, Wear: materials, mechanisms and practice, John Wiley & Sons, 2006.

[14] O. Vingsbo, S. Söderberg, On fretting maps, Wear, 126 (1988) 131-147.

[15] A. Ramalho, L.M. Correia, J.D. Costa, Fretting fatigue of zinc coated low carbon steel EN H320 M, Tribology International, 33 (2000) 761-768.

[16] H. Gao, H. Gu, H. Zhou, Sliding wear and fretting fatigue resistance of amorphous Ni-P coatings, Wear, 142 (1991) 291-301.

[17] R.B. Waterhouse, Fretting corrosion, Pergamon Press, Oxford; New York, 1972.

[18] K.J. Kubiak, T.W. Liskiewicz, T.G. Mathia, Surface morphology in engineering applications: Influence of roughness on sliding and wear in dry fretting, Tribology International, 44 (2011) 1427-1432.

[19] L. Thiery, L. Moui, J.J. Duprat, Performa 280.5, Coventya, UK, 2004.

[20] Coventya, Protection : Technical sheets and documentation, Coventya, France, 2013.

[21] W.C. Oliver, G.M. Pharr, An improved technique for determining hardness and elastic modulus using load and displacement sensing indentation experiments, Journal of Materials Research, 7 (1992) 1564-1583.

[22] C.S. Lin, H.B. Lee, S.H. Hsieh, Microstructure and formability of ZnNi alloy electrodeposited sheet steel, Metallurgical and Materials Transactions A: Physical Metallurgy and Materials Science, 31 (2000) 475-485.

[23] T. Sasaki, Y. Hirose, Residual stress distribution in electroplated Zn・Ni alloy layer determined by X-ray diffraction, Thin solid films, 253 (1994) 356-361.

[24] Y. Berthier, L. Vincent, M. Godet, Fretting fatigue and fretting wear, Tribology International, 22 (1989) 235-242.

[25] ASTM, F519-10, Standard Test Method for Mechanical Hydrogen Embrittlement Evaluation of Plating/Coating Processes and Service Environments1, ASTM International, Pennsylvania, USA.

[26] S. Fouvry, P. Kapsa, L. Vincent, Quantification of fretting damage, Wear, 200 (1996) 186-205.

[27] L. Vincent, Y. Berthier, M. Dubourg, M. Godet, Mechanics and materials in fretting, Wear, 153 (1992) 135-148.

[28] S. Fouvry, P. Kapsa, L. Vincent, Analysis of sliding behaviour for fretting loadings: determination of transition criteria, Wear, 185 (1995) 35-46.

[29] Y. Berthier, L. Vincent, M. Godet, Velocity accommodation in fretting, Wear, 125 (1988) 25-38.

[30] H. Kurita, H. Yamagata, Effect of hardness on fretting wear characteristics of AC9B and AC8A aluminum alloys, Nippon Kinzoku Gakkaishi/Journal of the Japan Institute of Metals, 62 (1998) 50-55.

[31] R. Ramesh, R. Gnanamoorthy, Effect of hardness on fretting wear behaviour of structural steel, En 24, against bearing steel, En 31, Materials and Design, 28 (2007) 1447-1452.

[32] X. Zhang, H. Liu, X.s. Wang, On the effects of hardness on the fretting wear behavior and on the wear debris composition of carbon steel, Mocaxue Xuebao/Tribology, 15 (1995) 300-305.

[33] L. Vincent, Y. Berthier, M.C. Dubourg, M. Godet, Mechanics and materials in fretting, Wear, 153 (1992) 135-148.